ACIDIC AQUEOUS URANIUM ELECTRODEPOSITION FOR TARGET FABRICATION

## A.M. Saliba-Silva[1], E. T. Oliveira[1], R. H. L. Garcia[1], M. Durazzo[1]

[1] Centro do Combustível Nuclear - Instituto de Pesquisas Energéticas e Nucleares IPEN/CNEN
Av. Prof. Lineu Prestes, 2242 Cidade Universitária,
São Paulo (SP) Brazil - CEP 05508-000
saliba@ipen.br

ABSTRACT

Direct irradiation of targets inside nuclear research or multiple purpose reactors is a common route to produce ^{99}Mo-^{99m}Tc radioisotopes. The electroplating of low enriched uranium over nickel substrate might be a potential alternative to produce targets of ^{235}U. The electrochemistry of uranium at low temperature might be beneficial for an alternative route to produce ^{99}Mo irradiation LEU targets. Electrodeposition of uranium can be made using ionic and aqueous solutions producing uranium oxide deposits. The performance of uranium electrodeposition is relatively low because a big competition with H_2 evolution happens inside the window of electrochemical reduction potential. This work explores possibilities of electroplating uranium as UO_2^{2+} (Uranium-VI) in order to achieve electroplating uranium in a sufficient amount to be commercially irradiated in the future Brazilian RMB reactor. Electroplated nickel substrate was followed by cathodic current electrodeposition from aqueous $UO_2(NO_3)_2$ solution. EIS tests and modeling showed that a film formed differently in the three tested cathodic potentials. At the lower level, (-1.8V) there was an indication of a double film formation, one overlaying the other with ionic mass diffusion impaired at the interface with nickel substrate as showed by the relatively lower admittance of Warburg component.

1. INTRODUCTION

Alpha spectroscopy uses commonly nitric uranyl electrodeposition [1, 2] to evaluate uranium content in mineralogical analysis. Another possible area for uranium electrodeposition is the manufacturing of irradiation targets to produce the radionuclides ^{99}Mo and ^{131}I under neutrons bombarding in nuclear research reactors. Both radionuclides are produced by ^{235}U fission [3]. In special, there is a vital radionuclide for nuclear medicine that is mostly used for cancer diagnosis, which is the metastable technetium-99m (^{99m}Tc). It has a half-life of 6.03h that emits a convenient gamma ray at 140.5keV [4]. This radionuclide is produced as a decay of molybdenum-99 (^{99}Mo), having a half-life of 65.9h. As shown, schematically in Figure 1.
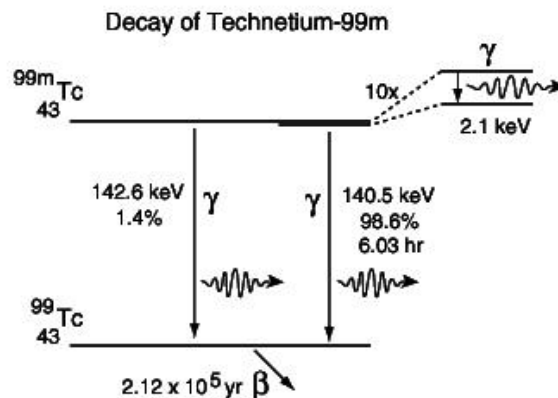
Figure 1: Decay of ^{99m}Tc and the emission of 140.5 keV of gamma ray, having a half-life of 6.03h [4]

The present technological challenge is to deposit electrochemically sufficient amount of uranium compound to produce the irradiation targets containing up to 20 wt% of ^{235}U (LEU – Low Enriched Uranium) [5] since electrodeposition of uranium is a viable route [6]. As summarized by Santos et al [7], the uranium electrodeposition in NH_4Cl medium produces films containing uranyl groups isolated or linked to other uranyl groups. They found that the reduction of H^+ ions was relevant during the process, and the solution becomes more alkaline at cathode proximity. These results support the results published by Wheeler et al. [8] suggesting that the electrodeposition can develop a polymerized structure under hydrolysis with increasing pH. The precipitation of uranium compound occurs when the polymerization reaches the solubility product of the species in solution. A UO_3 hydrate is then deposited from the electrolyte as a hydrated polymeric compound containing oxygen bridges in the chain.

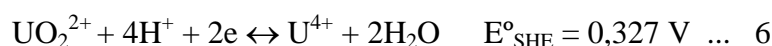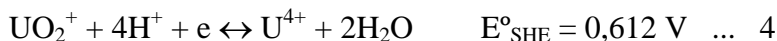Electrochemically, the expected reaction producing oxide deposit is [9]:

$$U^{3+} + 2H_2O = UO_2 + 4H^+ + e^- \quad E^o_{SHE} = -0.382 - 0.2364.pH - 0.0591.\log[U^{3+}] \quad ... \quad 1$$
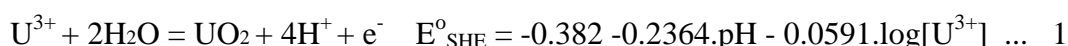
It depends on the electrochemical reaction of uranium-III generation from uranium-IV given by:

$$U^{4+} + e^- = U^{3+} \qquad E^\circ_{SHE} = -0.607 \text{ V} \quad ... \quad 2$$

This reaction may be associated with uranium and aqueous solution. Then, uranium-III would form hydroxyl compound, in acidic media, given by the following reaction:

$$U^{3+} + H_2O = UOH^{3+} + H^+ + e^- \qquad E^o_{SHE} = -0.538 - 0.0591.pH \text{ V} \quad ... \quad 3$$

Uranyl ion ($UO2^{2+}$), which is Uranium-VI, could undergo a reduction process to Uranium-V, which is unsteady and promptly reduces to Uranium-IV in acidic media. Cathodic polarization may favor the reduction [9] as suggested by the following reactions:

$$UO_2^+ + 4H^+ + e \leftrightarrow U^{4+} + 2H_2O \qquad E^o_{SHE} = 0,612 \text{ V} \quad ... \quad 4$$

$$UO_2^{2+} + e \leftrightarrow UO^{+2} \qquad E^o_{SHE} = 0,062 \text{ V} \quad ... \quad 5$$

$$UO_2^{2+} + 4H^+ + 2e \leftrightarrow U^{4+} + 2H_2O \qquad E^o_{SHE} = 0,327 \text{ V} \quad ... \quad 6$$

A Pourbaix diagram was calculated for UO_2^{2+} [50mM] in aqueous solution using Medusa software [10] and is presented in Figure 2.
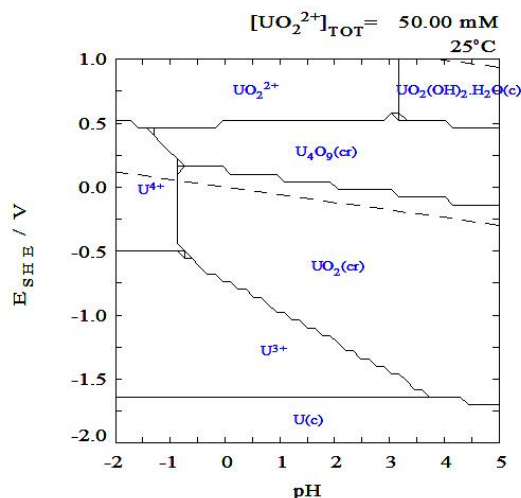
Figure 2 – Calculated Pourbaix Diagram for the system UO_2^{2+} [50mM] in aqueous solution using Medusa Software[10].

In the present study, we performed experiments using direct cathodic polarization to promote uranium electrodeposition in order to examine the possibility to use this process for preparing irradiation targets.

2.   EXPERIMENTAL

The electrochemical cell for uranium electrodeposition was a vertical quartz tube, supported by a polypropylene structure, containing the electrolyte solution inside the cell, which was closed at the bottom by the sample at cathode opening. The sealing was made by rubber O-ring covered with Teflon band. The experimental device exposed 2 cm^2 of cathodic area to the electrolyte. The reference electrode, which was used in all experiments, was Ag/AgCl. AA6061 aluminum alloy coupons were used as a base for Ni-substrate electrodeposited. These AA6061 coupons were heat treated at 450ºC during 1 hour for full recrystallization of aluminum, cooled till room temperature and then ground with emery paper #600, rinsed with NaOH for 2 minutes and duly degreased with acetone. All aluminum coupons were electroplated with nickel (Watts solution; -1.5 $V_{Ag/AgCl}$; 600s), rinsed and then assembled in the cathode. To perform the uranium electrodeposition, 30 ml of uranyl solution was poured into the cell. Platinum was used as counter electrode. The cathodic polarization was followed by chronoamperometric measurements at 3 levels: -1.8, 2.0 and −2.2 $V_{Ag/AgCl}$ during 600s; the electrolyte temperature was maintained at 30ºC. No electrolyte stirring was introduced. Each test had 3 replications of uranium electrodeposition to check the reproducibility.

3.   RESULTS AND DISCUSSIONS

The microstructures from the experiments had a typical appearance shown in Figure 3. Figure 3a. shows the microstructure of nickel substrate and Figure 3b. shows a typical electrodeposited film.

(a)   (b)
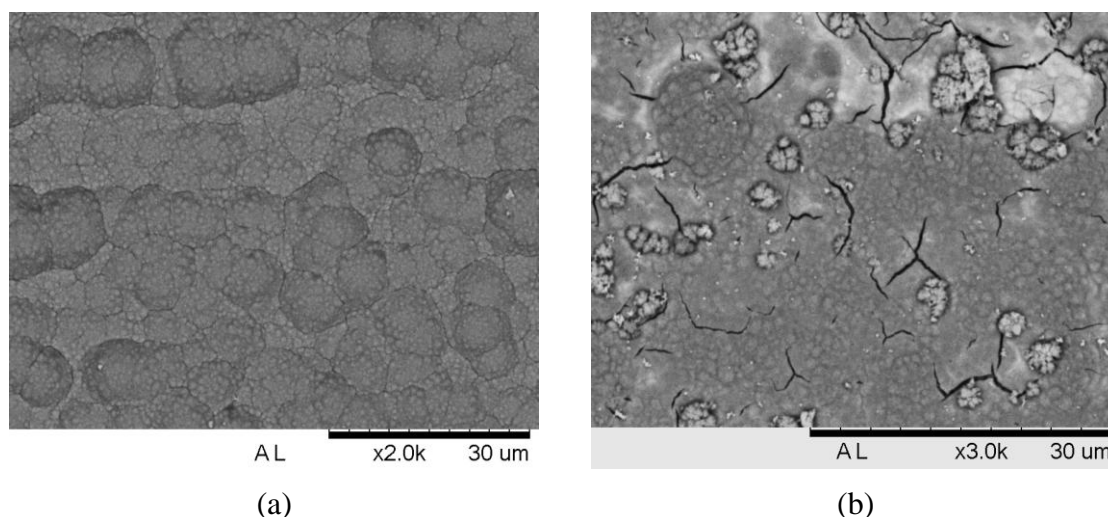
Figure 3 – SEM micrographs representation of room temperature dried surfaces of:
(a) nickel electrodeposited substrate microstructure;
(b) nickel substrate microstructure and uranium electrodeposition from 50 mM
UO$_2$(NO$_3$)$_2$ aqueous electrolyte, during 600s at 30 ºC at -2V.

Tree-type structures emerged from specific areas during the layer formation suggesting that a particular crystallization occurred simultaneously with film deposition of uranyl compound. Some cracks developed over the electrodeposit film in a fragile way, which should be more deeply investigated in future works.

As already previously described, the formation of uranyl film is thought to be formed by the electrochemical followed by chemical precipitation to form the uranium deposited film. Nevertheless, in acidic media, aqueous electrolysis is prone to happen at cathode promoting localized anodic oxygen evolution at the cathode by 4 electrons transfer:

$$2H_2O \rightarrow 4H^+ + O_2 + 4e^- \qquad E^0 = -1,230 \ V_{SHE} \qquad ... \ 1$$

This reaction may be catalyzed by electrochemical oxidation of multivalent metal [11], which is the case of UO_2^{2+}. It is also believed that, in acidic solutions, aqueous electrolysis may also happen in localized anodic regions at the cathodes, producing H_2 and OH^- by:

$$2H_2O + 2e^- \rightarrow H_2 + 2OH^- \qquad E^0 = -0,827 \ V_{SHE} \qquad ... \ 2$$
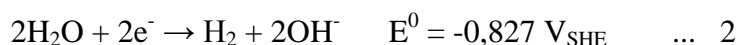
So this electrolytic mechanism allows OH^- to capture the UO^{2+} (Uranium-VI) to form hydroxides as uranyl hydroxide/oxide deposition by chemical precipitation of uranyl compounds over cathode surface.
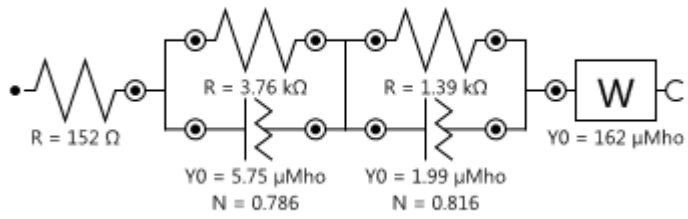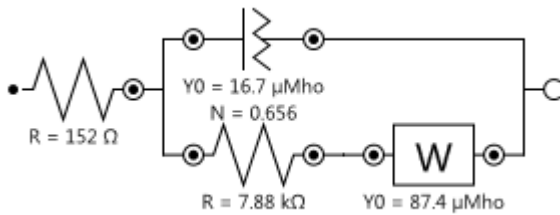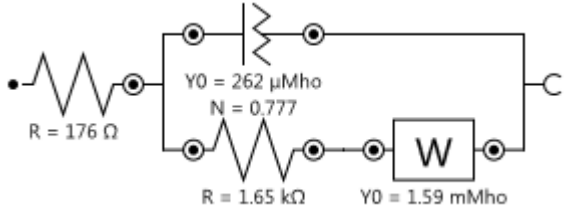
The structure of the deposited uranyl compound, as shown in Figure 3b, had a seemingly opened appearance towards its base in contact with the substrate due to cracks during drying. Nevertheless it showed, under several EIS tests, resistive properties for this layer, depending on the level of cathodic potential as shown in the Figure 4.

(a)

(b)

(c)
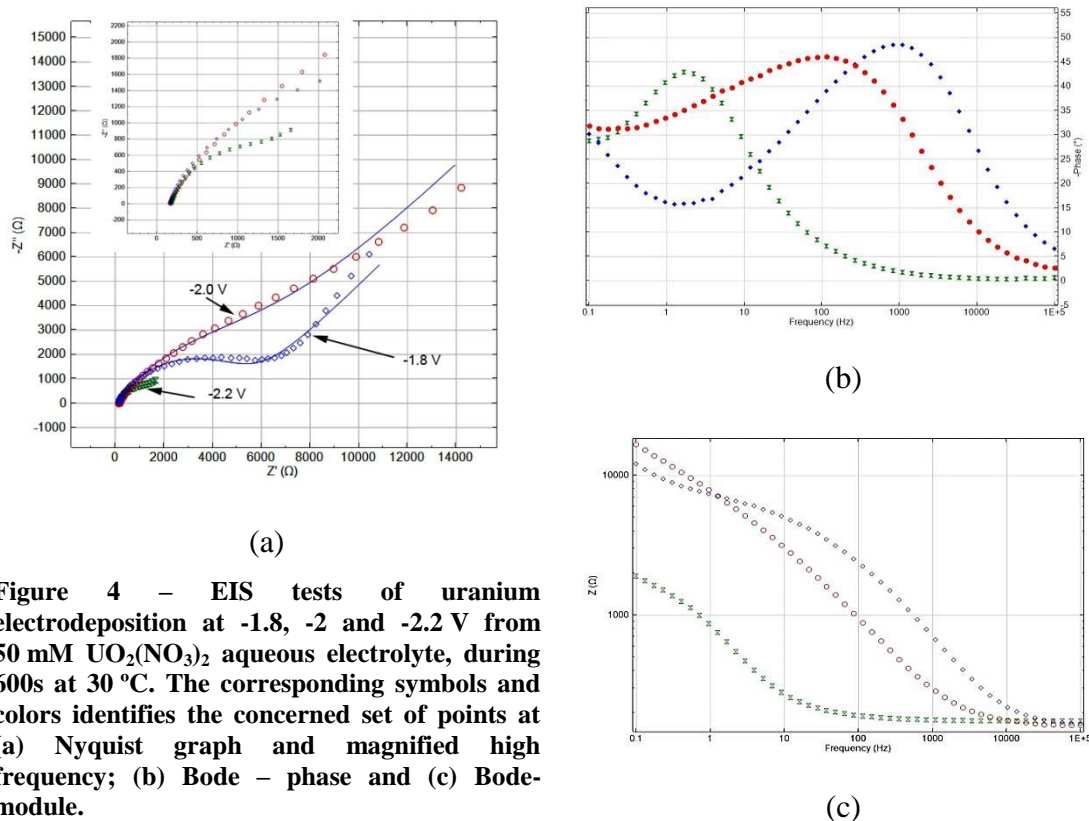
Figure 4 – EIS tests of uranium electrodeposition at -1.8, -2 and -2.2 V from 50 mM $UO_2(NO_3)_2$ aqueous electrolyte, during 600s at 30 ºC. The corresponding symbols and colors identifies the concerned set of points at (a) Nyquist graph and magnified high frequency; (b) Bode – phase and (c) Bode-module.

From these EIS graphs, it is possible to see that cathodic potential provided different layer characteristics. In Nyquist diagram, the −1.8 V graph gave a response displaying a pronounced deformed circle, which presented as an elongated plateau parallel to the real axis. This is characteristic of a probable formation of convoluted circles due to probably formation of two layers, one on the top of the other. The Warburg segment following this plateau at lower frequencies is highly significant at this level of cathodic potential. It indicates a diffusion component of involved ionic species inside the formed layer near to the substrate interface. These characteristics are pertinent to EIS results, and they are described in other studies of chemical conversion [12-14] and paintings [15]. As the cathodic voltage increased to higher values (−2.0 V and −2.2 V), the two-layer model changed drastically to another model of a single layer. The voltage increase to −2.2 V produced a less resistive uranium electrodeposited film. All this sequence of EIS equivalent circuit modeling can be followed in Table 1. The χ^2 probability of the models during calculating iteration acquired reliable statistical significance, which resembles fairly robust modeling.

Table 1 – EIS equivalent Circuits measured for the 3 used cathodic potential −1.8, −2.0 and −2.2 V for uranium electrodeposition.

Cathodic Potential	Equivalent Circuit	χ^2
-1.8 V		0.016
-2.0 V		0.053
-2.2 V		0.016

The best model fitting was achieved by using the component CPE (constant phase element).

This component is independent of frequency and represented by $Q = 1/Y_0(j\omega)^n$, where Y_0 is the admittance of CPE, $j^2 = -1$ (complex number unit) and ω is the phase angle. If n=1, then CPE represents a perfect capacitor and if n=0 a pure resistor. As could be interpreted in the supplied equivalent circuit at −1.8 V, there is a suggestion of two overlapping films, with 2 independent circuits in series. Either of them has its own circuit [RQ], one internal (very near to the cathode substrate) and the external one is exposed to the electrolyte. The Warburg component also appeared to be linked to the structure of the electrodeposition. It is a particular case of CPE when n = ½, and in the isotropic Nyquist diagram, at high frequency region, it forms a 45° inclined line. It is interpreted for the present case as the electrochemical activity at pore tips near the interface of the uranium deposited compound to the nickel substrate. The Warburg behavior shows by its considerably low admittance (Y0) at −1.8 V, that there is a closing pores condition at substrate interface, by sealing the conductive pore structure and impairing the ionic mass transfer by diffusion. In the modeled equivalent circuits at higher cathodic polarization, the two film structure becomes a single film having a Warburg component in series with the double layer resistance. It can be seen that there is a fall of 5 times in the double layer resistance from the cathodic polarization at −2.0 to −2.2 V. The Warburg admittance increased in more than 18 times. These evidences show that physically the resistance and thickness of the formed uranyl film lowered as the cathodic potential increased in this range.

4. CONCLUSIONS

There is a complex scenario of uranium redox reactions during electrodeposition. These reactions may vary due to different electrolytes and electrochemical conditions. Using acidic solution with pH at −1 level, no metallic uranium electrodeposition was observed. Most likely the electrodeposition, in acidic electrolyte, is dependent on aqueous electrolysis producing floating localized anodic regions at the cathode, where a large amount of formed hydroxyl promotes the electrodeposition of uranium oxides compounds at the cathode surface, direct from uranyl (Uranium-VI). EIS tests and modeling showed that a film formed differently in the three tested cathodic potentials. At -1.8V there is an indication of a double film formation, one overlaying the other with ionic mass diffusion impaired at the interface of the uranium deposited film with nickel substrate, as showed by relatively lower admittance of Warburg component. This indicated that a sealing over the structure took place during the electrodeposition process. At higher cathodic potentials, the EIS model changed. It implies a decrease in film thickness by lowering the resistance of double layer. The constant phase element showed an increase of the capacitive contribution to the film as the cathodic potential increased, indicating more active porosity of the uranium electrodeposited film, leading this potential to produce less effective electrodeposition of uranium compounds films, which do not help the increase of uranium electrodeposition to produce irradiated targets.

5. ACKNOLEDGEMENTS

6. REFERENCES

1. Crespo, M.T., "A review of electrodeposition methods for the preparation of alpha-radiation sources*." Appl Radiat Isot*, 2012. **70**(1): pp. 210-5.
2. Hallstadius, L., "A method for the electrodeposition of actinides*." Nuclear Instruments & Methods*, 1984. **223**: pp. 266-2678.
3. Saliba-Silva, A.M., et al., "Uranium Briquettes for Irradiation Targets", in *2011 International Nuclear Atlantic Conference -(INAC)* 2011, Associação Brasileira de Energia Nuclear - ABEN: Belo Horizonte, MG.
4. HyperPhysics, G. *Technetium-99m.* [cited 2013 Feb, 06 2013]; Available from: http://hyperphysics.phy-astr.gsu.edu/hbase/nuclear/technetium.html.
5. National Research Council, C., "Medical isotope production without highly enriched uranium", C. National Research Council, Editor 2009, National Academies Press.
6. Thied, R.C., et al., "Process for separating metals - US 6,911,135", in *United States Patent*, U.S. Patent, Editor 2005: US.
7. Santos, L.R., M.E. Sbampato, and A.M.d. Santos, "Characterization of electrodeposited uranium films*." Journal of Radioanalytical and Nuclear Chemistry*, 2004. **261**(1): pp. 203-209.
8. Wheeler, V.J., R.M. Dell, and E. Wait, "Uranium trioxide and the UO3 hydrates*." Journal of Inorganic and Nuclear Chemistry*, 1964. **26**(11): pp. 1829-1845.
9. Xu, Y., "Electrochemical Treatment of Metal-Bearing Aqueous Waste Based on Novel Forms of Carbon", in *College of Engineering and Mineral Resources* 1999, West Virginia University: Morgantown, Vi.
10. Puigdomenech, I., "MEDUSA", 2009, Royal Institute of Technology: Stockholm, Sweden. p. Software to calculate equilibrium diagrams.
11. Wendt, H. and R. Gerhard, *Electrochemical Engeneering: Science and Technology in Chemical and Other Industries*. 1999, Berlin: Springer.
12. Saliba-Silva, A., et al., "Improving the corrosion resistance of NdFeB magnets: an electrochemical and surface analytical study*." Surface & Coatings Technology*, 2004. **185**(2-3): pp. 321-328.
13. Saliba-Silva, A.M., et al., "Corrosion protection of sintered NdFeB magnets by phosphating*." Surface Treatment V: Computer Methods and Experimental Measurements*, 2001. **6**: pp. 65-74.
14. Saliba-Silva, A.M. and I. Costa, "Corrosion protection of a commercial NdFeB magnet by phosphating*." Advanced Powder Technology Ii*, 2001. **189-1**: pp. 363-368.
15. Walter, G.W., "A review of impedance plot methods used for corrosion performance analysis of painted metals*." Corrosion Science*, 1986. **26**(9): pp. 681-703.